Molecular and cellular responses to renal injury : a (phospho)-proteomic approach

Graauw, M. de

Annexin A2 phosphorylation in cell scattering

Chapter 6

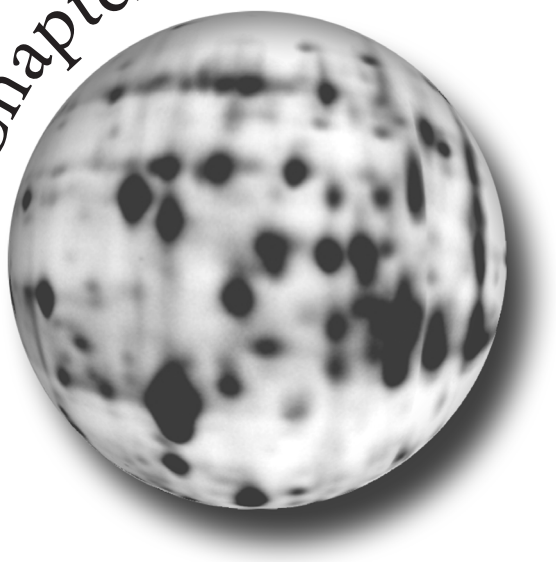

Annexin A2 tyrosine phosphorylation induces cell scattering and branching morphogenesis via cofilin activation

Marjo de Graauw[1], Ine Tijdens[1], Mirjam B. Smeets[2], Jean Paul ten Klooster[3], Peter L. Hordijk[3], André M. Deelder[2] and Bob van de Water[1]

[1]*Division of Toxicology, Leiden/Amsterdam Center for Drug Research, Leiden University, P.O. Box 9502, 2300 RA, Leiden, The Netherlands. and* [2]*Biomolecular Mass Spectrometry Unit, Department of Parasitology, Leiden University Medical Center, P.O. Box 9600, 2300 RC Leiden, The Netherlands and* [3]*Sanquin Research at CLB, Department of Molecular Cell Biology, 1066 CX Amsterdam, The Netherlands*

ABSTRACT

Dynamic remodelling of the actin cytoskeleton is required for cell adhesion, motility and migration and can be regulated by tyrosine kinase activity. We identified phosphorylation of the lipid-, calcium-, and actin-binding protein, annexin A2 (AnxA2) at Tyr23 as a primary event preceding v-Src kinase-induced cell scattering and migration. Expression of the phospho-mimicking mutant, Y23E-AnxA2 was sufficient to induce actin reorganization and cell scattering. This was dependent on PI-3 kinase and MEK activity. RNAi-mediated knock-down of AnxA2 resulted in increased stress fiber formation and inhibition of cell scattering. In a 3D branching morphogenesis assay WT-AnxA2 cysts only developed branches in the presence of HGF while, Y23E-AnxA2 induced HGF-independent branching morphogenesis. The Y23E-AnxA2-induced morphology is associated with dephosphorylation/activation of the actin-severing protein, cofilin. Together our findings point to an important role for AnxA2 phosphorylation in the regulation of cytoskeletal dynamics during cell scattering and branching morphogenesis.

INTRODUCTION

The epithelial mesenchymal transition (EMT) is a highly conserved and important process regulating morphogenesis, tissue restructuring and tumour progression in multi-cellular organisms [1,2]. The transition process is characterized by loss of cell-cell interaction in association with an active, well-controlled rearrangement of the F-actin cytoskeletal network. In time, epithelial cells acquire a scattered and highly motile morphology that is appropriate for migration in an extra-cellular environment.

The onset of epithelial cell scattering is, amongst others, controlled by receptor tyrosine kinases, like the hepatocyte growth factor (HGF) receptor c-Met [2]. In addition to cell scattering, HGF induces branching morphogenesis of cells when cultured in three-dimensional collagen gels [3]. HGF-triggered signalling downstream of c-Met is mediated by non-receptor tyrosine kinases such as Src kinase family members [4]. Activated Src kinase causes tyrosine phosphorylation (pTyr) of various cellular proteins, including cytoskeletal and cell adhesion proteins that can influence the adhesive phenotype of epithelial cells [5-7]. Most likely, these Src phosphorylated adhesion and/or cytoskeleton-regulating proteins mediate the onset of cell scattering and EMT. Therefore, a phospho-tyrosine proteome-wide characterization of Src kinase substrates and candidate EMT regulating proteins is required.

To identify Src substrates that may mediate the onset of cell scattering, we used conditional v-Src kinase-induced scattering of MDCK cells [5] in combination with phospho-tyrosine proteomics. We identified phosphorylation of annexin A2 (AnxA2) as the primary event preceding Src kinase-induced actin remodelling and cell scattering. Annexins are a large family of Ca^{2+}-binding proteins characterized by their ability to interact with negatively charged membrane surfaces [8]. Structurally, annexins consist of a conserved carboxy-terminal core domain and a variable N-terminal domain. For AnxA2, this N-terminal tail domain harbours a highly specific binding site for the small dimeric protein S100A10 and phosphorylation sites for different kinases (*e.g.* Ser25 for PKC phosphorylation and the Tyr23 for Src kinase phosphorylation) [9,10]. Recent RNAi approaches indicate a role for AnxA2 in regulating endocytotic and exocytotic processes as well as cell-cell junction formation and actin dynamics [11, 12-15]. AnxA2 as well as the close family member AnxA1 bind F-actin [16]. For AnxA2, bundling of F-actin is regulated by the S100A10-mediated tetramer formation [17-19]. Src kinase-mediated phosphorylation of this AnxA2 tetrameric complex completely inhibits its ability to bind or bundle F-actin in vitro [20]. This suggests that Src-dependent phosphorylation of AnxA2 may regulate the cytoskeletal dynamics necessary for Src-dependent processes, such as EMT. Thus far, the role of tyrosine phosphorylated AnxA2 in the regulation of cell-cell adhesions and F-actin organization in the context of cell scattering and EMT is not known.

Here we determined the role and mechanism of tyrosine phosphorylated AnxA2 in EMT-related processes. We observed that expression of a phospho-mimicking mutant of AnxA2 (Y23E-AnxA2) is sufficient to induce F-actin reorganization, enhanced cell scattering and protrusion formation as well as formation of tubules in a branching morphogenesis assay independent of HGF. AnxA2 was also required for cell scattering and

tubulogenesis. Y23E-AnxA2 induced dephosphorylation (*i.e.* activation) of the actin severing protein cofilin, whereas phosphorylated cofilin inhibited AnxA2 phosphorylation-mediated cell scattering. Our results indicate a role for AnxA2 phosphorylation in the regulation of cofilin activity in the context of both two- and three-dimensional cellular restructuring processes.

MATERIALS AND METHODS

Cell treatment conditions

Madin Darby Canine Kidney (MDCK) cells were maintained in DMEM supplemented with 10% (v/v) FCS and penicillin/streptomycin at 37 °C in a humified atmosphere of 95% air and 5% carbon dioxide. The ts-v-Src MDCK cell line was generated by R. Friis 5. For experiments, these cells were cultured at 40 °C for 20 hours and shifted to 35 °C for 0 to 24 hours to activate Src kinase. For preparation of stable Annexin A2 expressing cell lines or RNAi cell lines, MDCK cells were transfected with 0.8 μg DNA of pGFP, pGFP-AnxA2 WT and pGFP-AnxA2 Y23E (gift from Dr. V.Gerke, Institute of Medical Biochemistry, Muenster), pSUPER-empty or pSUPER-shAnxA2 (A; TGACGCTTCTGAACTGAAA and B: GAACTTGCATCAGCATTGA) using Lipofectamine-Plus reagent according to the manufacturer's procedures (Life Technologies, Inc). Stable transfectants were selected using 800 μg/ml G418. Individual clones were picked and maintained in complete medium containing 100 μg/ml G418. Clones were analyzed for AnxA2 and GFP expression using Western blotting and immunofluorescence. For further experiments up to three stable cell lines were used per construct.

1D and 2D gel electrophoresis and Western blotting

1D gel electrophoresis was performed as described previously [21]. For 2D protein separation, 24 cm immobilized pH gradient (IPG) strips pH 3-10 NL (GE Healthcare) were rehydrated with urea protein samples (as described previously [21]) at 30V for 12 hours. Isoelectric focusing was performed at room temperature using the Ettan IPGphor IEF system (GE Healthcare) and IPG strips were equilibrated for 10 min in equilibration buffer (6 M urea, 2% (w/v) SDS, 1% (w/v) DTT, 30 % (v/v) glycerol and 50 mM Tris pH 6.8). Equilibrated IPG strips were transferred onto 20x26 cm 9% SDS/PAGE gels. Gels were run overnight in a Hoeffer DALT 10 gel system (GE Healthcare) and either fixed in 30% MeOH / 7.5% Acetic Acid for subsequent Sypro ruby staining (Molecular Probes) or transferred to nitrocellulose membrane (Schleicher and Schuell) overnight at 4 °C. Both 1D and 2D blots were incubated with primary antibody overnight at 4 °C using GFP (Roche), PY99 (Santa Cruz) or AnxA2 (HH7, V. Gerke), followed by incubation with horseradish peroxidase conjugated secondary antibody (GE Healthcare) for 1h. Protein signals were detected with the ECL plus method (GE Healthcare) followed by scanning of the blots with a, Typhoon 9400 (GE Healthcare).

2D image analysis

Differences in tyrosine phosphorylation were detected by PDQuestTM 2D Gel Analysis Software (Bio-Rad Laboratory, Inc.). All phospho-tyrosine (PY) profiles were aligned with total protein profiles (Sypro ruby images) to mark proteins undergoing changes in tyrosine phosphorylation. Matched spots from triplicate blots that could be detected on the associated Sypro ruby stained gel were excised from the gel, digested with trypsin and subsequently identified by an Ultraflex time-of-flight mass spectrometer (Bruker Daltonics) equipped with a LIFT-MS/MS facility controlled by FlexControl 2.0 software package.

Immunofluorescence

For immuno-fluorescence studies cells were cultured on collagen coated glass coverslips in 24-well dishes. Cells were fixed with 3.7% formaldehyde for 10 min followed by 3 washes with PBS. After cell permeabilization and blocking with TBP (PBS, 0.2% (w/v) Triton X-100, 0.5% (w/v) bovine serum albumin, pH 7.4), cells were stained for β-catenin (Transduction Lab), PY418-Src (BioSource), PY99 (Santa Cruz) or myc (Roche) overnight at 4 °C and subsequently incubated with Alexa-488 or Cy-3 conjugated secondary antibody (Molecular Probes) in combination with rhodamin-phalloidin (Molecular Probes) to label the F-actin cytoskeletal network.

Scattering assay

For a scattering assay, cells were cultured in small clusters on collagen-coated coverslips overnight followed by an 8 h incubation with 50 ng/ml HGF (50 ng/ml, Moher B.V.). Thereafter cells were fixed and stained for immunofluorescence.

ECIS assay for cell attachment and wound healing

Cell attachment, spreading and wound healing was monitored using ECIS (Applied BioPhysics) [22]. The wells in the ECIS electrode arrays (8W1E, Applied BioPhysics) were coated with collagen (20 μg/ml) or fibronectin and 400 μl of cell suspension (1.5 x 105 cells per well) was added to each well. The wells were incubated overnight, while attachment and spreading were followed by means of online measurements of impedence.

Live-cell imaging

For live cell imaging, WT-AnxA2-GFP and Y23E-AnxA2-GFP cells were plated on tissue culture dishes containing a collagen-coated coverslip and maintained at 37 °C in 5 % CO2 in a climate control unit on a Nikon Eclipse TE2000-U inverted microscope. Images were typically taken at 5 min interval using a Bio-Rad Radiance 2100 confocal system with a 60 X Plan Apo (NA 1.4; Nikon) objective lens. Image acquisition was controlled using the Laser Sharp software (Bio-Rad) in combination with an in house developed macro to avoid the auto-focus problem. Movies were processed with Image-Pro® Plus (Version 5.1; Media Cybernetics).

RESULTS

Phospho-proteomics of *ts*-v-Src cells identifies phosphorylation of AnxA2 as a primary event in cell scattering

Using phospho-proteomics we identified proteins that are differentially phosphorylated in relation to v-Src-induced cell-cell dissociation and scattering [5]. Ts-v-Src MDCK cells formed epithelial cell clusters at 40 °C (non-permissive temperature) (**Fig. 1A**). The F-actin cytoskeletal network consisted of predominantly a cortical actin ring and long, thin stress fibres. At 35 °C (permissive temperature), cells lost their cell-cell interaction and cell scattering was induced (**Fig. 1A**). This was preceded by reorganization of the F-actin cytoskeleton an increased protein tyrosine phosphorylation (pTyr) (**Fig. 1A-C**). Herbimycin A, an inhibitor of Src kinase family members, inhibited both increased pTyr as well as cell scattering (**Fig. 1B-C**).

Next, we screened for proteins that were tyrosine phosphorylated prior to v-Src-induced loss of AJs using 2D-phospho-tyrosine blotting. Phospho-tyrosine protein blots of cells cultured at 40 °C were compared with those of cells cultured at 35 °C for 2h (**Fig. 1D**), a time point at which protein pTyr was increased, while cells still exhibited cell-cell junctions (**Fig. 1A**). 25 protein spots with an increased pTyr were detected. Using MALDI-TOF-MS/MS twelve spots were positively identified (**Table 1**) and included: 1) transcription regulatory proteins, like ribonucleoprotein K and elongation factor 2; 2) heat shock proteins, like heat shock cognate 70 and 3) cytoskeleton regulatory proteins, like ezrin, radixin, cytokeratin 8 and 19, t-complex protein, annexin A1 (AnxA1), annexin A2 (AnxA2), vinculin and vimentin. AnxA2, ezrin and vinculin are known Src substrates [6,7,10,23], indicating the functionality of the phospho-proteomic analysis technique. Others are potentially novel Src kinase substrates. Many proteins are involved in the regulation of the F-actin cytoskeleton. AnxA2 was the major differentially pTyr protein in our screen, which was phosphorylated within 30 min of Src activation (**Fig. 1E**). Reprobing 2D blots for AnxA2 indicated that approximately 10 % of total AnxA2 was phosphorylated in response to Src activation (**Fig 1F**).

Y23E-AnxA2-GFP alters the F-actin cytoskeletal organisation

So far, the biological role of tyrosine phosphorylation of AnxA2 in cell migration and EMT-related processes, has not been studied. Tyr 23 of AnxA2 is phosphorylated by Src kinase [10]. To study the effect of phosphorylated AnxA2 on EMT-related processes, we used Y23E-AnxA2-GFP, in which the Tyr residue was replaced by a Glut residue, thereby creating a phospho-mimicking mutant. MDCK cell lines stably expressing GFP, WT-AnxA2-GFP or Y23E-AnxA2-GFP were created. WT- and Y23E-AnxA2 were expressed at low levels as compared to endogenous AnxA2 (data not shown). When cultured at high density, WT and Y23E-AnxA2 were both associated with the plasma membrane at sites of cell-cell interaction (**Fig. 2A**). The F-actin network of cells expressing WT-AnxA2 resembled that of control GFP-expressing cells. In contrast, Y23E-AnxA2 cells contained less F-actin stress fibers and those present were short, disorganized and often clustered

(**Fig. 2A**), suggesting an involvement of phosphorylated AnxA2 in F-actin organization.

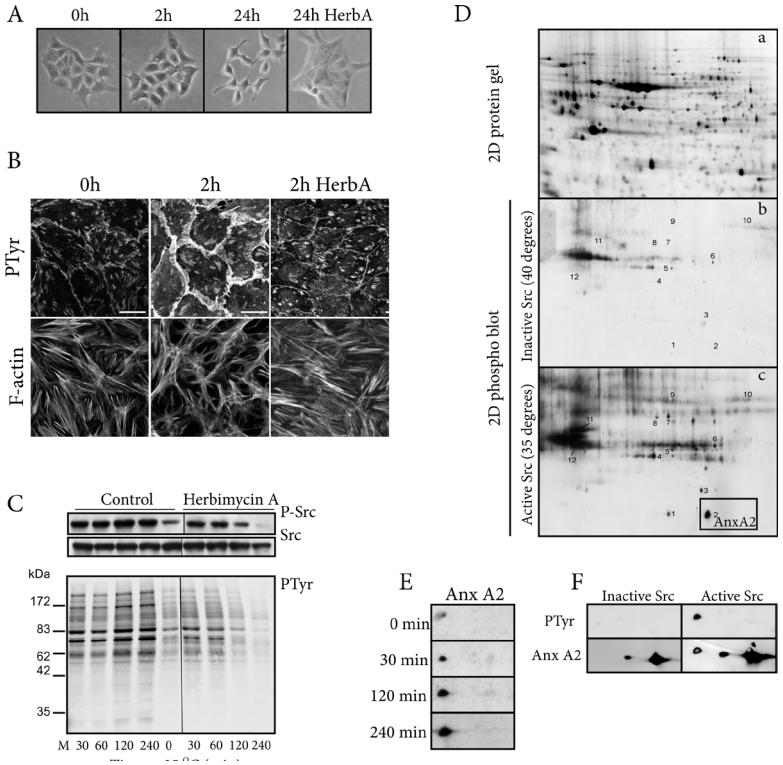

Figure 1. *Phospho-proteomic identification of AnxA2 as a phospho-substrate in Src kinase-induced scattering.* Ts-v-Src MDCK cells were shifted from the non-permissive temperature (40 ºC) to the permissive temperature (35 ºC) for 0, 2 and 24 h in the absence or presence of herbimycinA (1 μM). Cells were imaged using phase contrast (A) immuno-stained for pTyr (PY99) and F-actin followed by confocal laser scanning microscopy. (B) and analyzed for differential tyrosine phosphorylation and (P)-Src using 1D Western blotting (C). For phospho-protein identification four 2D gels were run per condition (40 ºC and 2 h at 35 ºC); one preparative Sypro ruby stained protein gel (a) and 3 gels for transfer of proteins to nitrocellulose membranes and staining for pTyr proteins (b,c) (D). Phosphorylation of AnxA2 was followed over time (E) 2D Blots were reprobed for AnxA2 to determine the amount of phospho-AnxA2 (F). All blots were run in triplicate and analyzed using PDQuest software followed by spot picking and MALDI-TOF-MS identification (See also **Table 1**). Bars, 20 μM.

Y23E-AnxA2-induced cell scattering is blocked by LY294002 and U0126

To investigate the role of phosphorylated AnxA2 in F-actin reorganization and cell scattering, Y23E-AnxA2 cells were cultured overnight at low density on either collagen (Cn), fibronectin (Fn) or laminin (Ln). GFP and WT-AnxA2 cells formed small islets on all three coatings. In contrast, Y23E-AnxA2 cells obtained a scattered morphology resembling that of Src kinase or HGF-induced scattering (**Fig. 2B**). Scattering was enhanced

on Cn and Fn, as compared to Ln, indicating that Y23E-AnxA2-mediated scattering is influenced by different ECM-conditions.

HGF-induced scattering is dependent on PI 3-kinase and MEK signalling [24-26]. To determine whether Y23E-AnxA2-induced scattering is dependent on PI 3-kinase (PI3K) or MEK signalling we used the PI3K inhibitor LY294002, which inhibited phosphorylation of the downstream target PKB and the MEK inhibitor U0126, which inhibited phosphorylation of the downstream target ERK1/2 (**Fig. 2D**). LY294002 and U0126 completely reversed the Y23E-AnxA2 phenotype; small islets for Y23E-AnxA2 cells, resembling those of WT-AnxA2 cells were formed in association with restoration of F-actin organization (**Fig. 2C**).

Table 1. *Data analysis of phospho-proteins spots subjected to MALDI-TOF-MS analysis*

Spot No.	Protein name	pI	Mw (kDa)	Swiss Prot AC	Protein function
1	Annexin A1	6.64	38.5	P04083	Cytoskeleton regulator
2	Annexin A2	7.56	38.4	P07355	Cytoskeleton regulator
3	Ribonucleoprotein K	8.67	51.2	NP_079555	(Post)-transcription regulator
4	Cytokeratin 19	5.05	44.1	P08727	Cytoskeleton regulator
5	Cytokeratin 8	5.52	53.5	P05787	Cytoskeleton regulator
6	t-complex protein	5.86	60.3	NP_036802	Chaperone/Cytoskeleton regulator
7	Ezrin	5.94	69.4	NP_003370	Cytoskeleton regulator
8	Radixin	6.03	68.6	AAA36541	Cytoskeleton regulator
9	Vinculin	5.51	123.6	P18206	Cytoskeleton regulator
10	Elongation factor 2	6.41	95.3	AAB60497	Transcription regulator
11	Heat shock cognate 70	5.07	72.3	NP_037215	Stress response
12	Vimentin	5.06	53.7	NP_112402	Cytoskeleton regulator

AnxA2 is important for cell adhesion, spreading and HGF-induced scattering

Since Y23E-AnxA2 caused cell scattering, we next determined whether AnxA2 itself has a functional role in cell spreading and scattering. For this purpose we generated AnxA2 knockdown MDCK cells using shRNA. Two different shRNA constructs were used. Compared to empty vector control cells (pSUPER) the levels of AnxA2 were greatly reduced in cells expressing either shRNA sequence A or B (pSUPER-AnxA2) as determined by Western blotting and immunofluorescence (**Fig. 3A**). The levels of the close family member AnxA1 were not altered (**Fig. 3A**). Next, we determined the effect of AnxA2 knock down on cell adhesion and spreading by plating both pSUPER and pSUPER-AnxA2 cells

on collagen. Within the same experiment either GFP or GFP-AnxA2 was reintroduced by transient transfection. Adhesion and spreading of the pSUPER-AnxA2 cells was inhibited compared to pSUPER control cells (**Fig. 3B**). Re-expression of GFP-AnxA2 WT in these pSUPER-AnxA2 cells rescued the phenotype and cells adhered and spread in a similar way as the pSUPER control cells (GFP positive cells in right panel **Fig. 3B**). Despite this clear involvement of AnxA2 in cell adhesion/spreading, 24 h after plating both pSUPER control and pSUPER-AnxA2 cells formed cell clusters (**Fig. 3C**). However, the F-actin organization was different between the two cell lines (data not shown). Thus, the absence of AnxA2 was associated with thicker and a more dense F-actin stress fiber network.

Next, we determined the role of AnxA2 in HGF-induced cell scattering. For this purpose cell clusters of pSUPER and pSUPER-AnxA2 cells were exposed to HGF for 8 h. The HGF-induced cell-cell disruption and cell scattering in pSUPER-AnxA2 cells was delayed, but not inhibited (**Fig. 3C-D**). Together these data demonstrate that annexin A2 is important in normal cell adhesion, spreading and scattering, possibly due to a diminished plasticity of the actin cytoskeleton and a reduction in its dynamics.

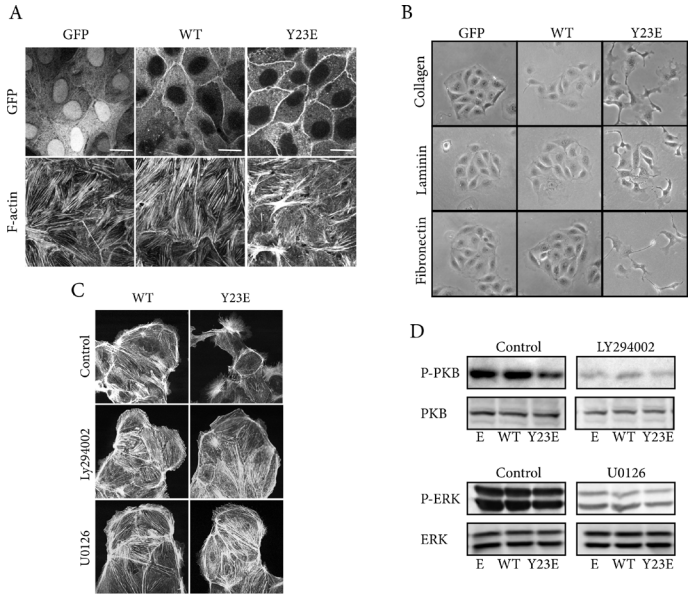

Figure 2. *Y23E-AnxA2-induced actin reorganization results in cell scattering, which is dependent on PI3K and MEK activity.* MDCK cells were stably transfected with GFP, WT-AnxA2-GFP or Y23E-AnxA2-GFP. Cells were plated on collagen-coated coverslips and after 24h fixated and imaged for GFP, AnxA2 and F-actin using confocal laser scanning microscopy. Bars, 20 μM (A). Cells were grown on collagen (Cn), fibronectin (Fn) or laminin (Ln) at low density and imaged with phase-contrast microscopy (B). Cell clusters were treated with the PI 3-kinase inhibitor LY294002 (2.5 μM) and MEK inhibitor U0126 (10 μM) for 24 h respectively and F-actin organization was analysed using immunofluorescent staining (C) and levels of phospho-PKB and phospho-ERK were analysed using Western blot analysis (D).

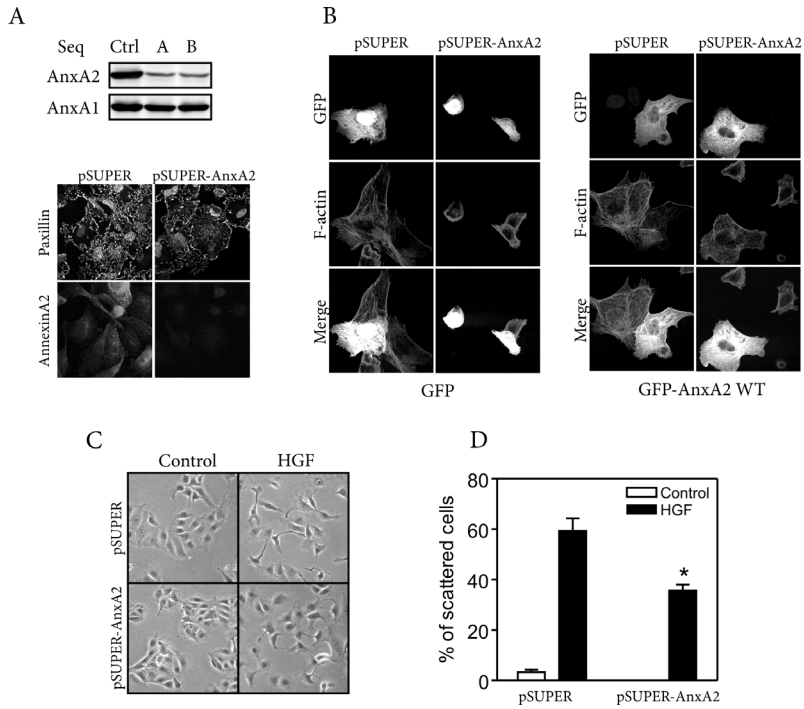

Figure 3. *RNAi-mediated depletion of AnxA2 inhibits cell adhesion and HGF-induced scattering.* MDCK cells were stably transfected with pSUPER shRNA vectors against AnxA2 (Seq A and B) or pSUPER empty vector control and analyzed for AnxA2 and AnxA1 expression by Western blotting and AnxA2 immunofluorescence using confocal laser scanning microscopy (A). Three clones for each construct (pSUPER control, pSUPER-AnxA2(A) and pSUPER-AnxA2(B)) were selected and pooled and used for further analysis. RNAi cells were transiently transfected with GFP or WT-AnxA2-GFP, followed by an adhesion assay on Cn-coated coverslips for 2 h; adherent cells were fixated and staining for F-actin followed by confocal laser scan microscopy of GFP and rhodamine-phalloidin (B). To determine the effect on cell scattering, RNAi and control cells were exposed to HGF (50 ng/µl) for 8 h (C). Cell scattering was determined by measuring the disruption of at least four cell–cell junctions per island (D).

Y23E-AnxA2 enhances cell adhesion and protrusiveness, but inhibits early adherens junction formation

Y23E-AnxA2 obtained a scattered phenotype on Cn or Fn when cultured at low density, despite the eventual formation adherens junctions at later time points when cultured at higher density. To get more insight in the differential behaviour of Y23E-AnxA2 cells compared to WT-AnxA2 cells we studied the spreading characteristics and AJ formation in more detail. First, the effect of Y23E-AnxA2 on the formation of AJs after cell spreading was determined by immunofluorescence staining. Cells were plated on collagen and allowed to adhere, spread and form AJ over a 24 h time-period. Y23E-AnxA2 enhanced cell adherence and spreading compared to WT-AnxA2 (**Fig. 4A**). During spreading, the Y23E-AnxA2 cells obtained a scattered phenotype, while WT-AnxA2 and GFP express-

ing cells were more rounded (**Fig. 4A** and data not shown). Moreover, while GFP and WT-AnxA2 cells formed β-catenin containing AJs within 2 h of plating, the phosphomimicking mutant did not. At 8 h most WT-AnxA2 cells had formed AJs, while this was partially the case for Y23E-AnxA2 cells. After 24h of adhesion all cells formed a confluent monolayer with β-catenin localization at AJs (**Fig. 4A**). However, the β-catenin-postive plasma membrane surface area was higher in WT-AnxA2 cells than in Y23E-AnxA2 cells.

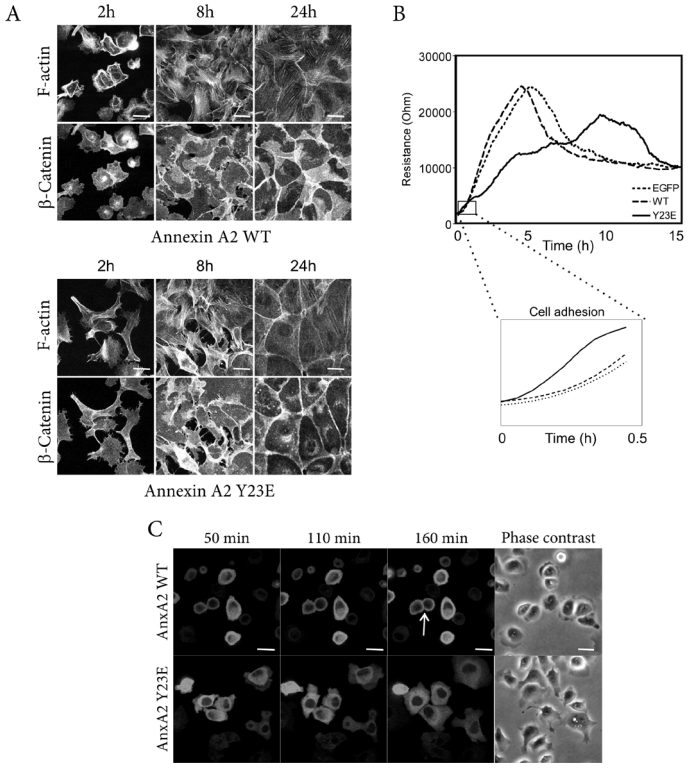

Figure 4. *Y23E-AnxA2 enhances cell adhesion and protrusiveness, but inhibits early adherens junction formation.* WT-AnxA2-GFP and Y23E-AnxA2-GFP expressing cells were plated on Cn-coated coverslips and after 2, 8 or 24h of adhesion fixated and stained for F-actin and β-catenin (A). To measure changes in resistance during a 15 h time period cells were plated on ECIS electrodes. Changes in resistance during the first 30 min after plating are presented in a zoomed graph (B). To study cellular dynamics live cell imaging was performed during the first 3 h of cell adhesion (C). Bars, 20 μM. Data are representative of three independent experiments.

To get more quantitative information of the dynamics of AJ formation, the differences in the spreading characteristics and AJ formation between WT- and Y23E-AnxA2 cells were also monitored continuously over a 15 h time period using electrical cell substrate impedance sensing (ECIS) (**Fig. 4B**). As cells attach and spread on the electrode surface, the effective area available for current flow is influenced resulting in an increase in re-

sistance 22. WT-AnxA2 and GFP cells exhibited an increase in resistance in the first 5h (**Fig. 4B**) related to cell spreading and formation of AJs. After reaching a peak, the resistance dropped to an intermediate value, marking a point where cells formed a confluent monolayer containing tight AJs (compare with 8 h in **Fig. 4A**). Y23E-AnxA2 cells showed a steeper increase in the first 30 minutes (**Fig. 4B**, zoom), which paralleled a faster cell adhesion and spreading. However, thereafter, the increase in resistance of Y23E-AnxA2 cells was slower compared to WT-AnxA2 cells and only reached peak levels after 10 h. This coincided with incomplete AJ formation at 8 h (**Fig. 4B**). After 10 h, the resistance drops for all cell lines as a result of the formation of a confluent monolayer.

The above data indicate that despite the fact that Y23E-AnxA2 had an increased efficiency to adhere, AJ formation was inhibited in these cells. We reasoned that this could be due to increased cell dynamics and enhanced formation of lamellipodia in these cells, resulting in a diminished possibility to form E-cadherin-based cell-cell junctions. To study this possibility, we performed live cell imaging of the early cell adhesion events (first 75 min) after plating either WT-AnxA2 or Y23E-AnxA2 cells. (**Fig. 4C**). Early after adhesion, WT-AnxA2 cells did not form extensive membrane ruffles. In addition, cells that were in close proximity to one another readily formed cell-cell interactions (**Fig. 4C**, indicated by an arrow). In contrast, Y23E-AnxA2 cells obtained a scattered phenotype early after adhesion, with the formation of many dynamic lamellipodia per cell. In some cells, Y23E-AnxA2 seemed to rapidly localize in newly formed lamellipodia. Although some Y23E-AnxA2 expressing cells were in close proximity to one another at the start of spreading, they did not form AJs. Together these data show that the phospho-mimicking mutant of AnxA2 stimulated cell spreading as well as the formation and dynamics of lamellipodia, thereby affecting stable AJ formation in MDCK cells early after adhesion.

In addition, given the role of AnxA2 in HGF-induced scattering and the induction of cell scattering by Y23E-AnxA2 we anticipated that phosphorylation of AnxA2 would affect recovery from an artificial wound. In a wound-healing assay using ECIS, we found that Y23E-AnxA2 expressing cells were able to close an artificial wound faster than cells expressing either WT-AnxA2 or GFP (data not shown).

Y23E-AnxA2 induces three dimensional branches independent of HGF

The scattering phenotype associated with the expression of Y23E-AnxA2 is reminiscent the EMT phenotype that is also observed with HGF. EMT processes are essential for the formation of multicellular structures [27]. Likewise, HGF induces a three-dimensional branching morphogenesis process in MCDK cells when cultured in collagen gels. To investigate AnxA2 phsophorylation is branching morphogenesis, GFP cells and cells expressing WT-AnxA2 or Y23E-AnxA2 were examined in three-dimensional collagen type 1 gels. In the absence of HGF only round cysts were observed with WT-AnxA2 cells similar to GFP control cells. In contrast, with Y23E-AnxA2 cells round cysts were only observed in ~50% of the structures. Yet, ~20% of the Y23E-AnxA2 cysts contained membrane protrusions on the outside (**Fig. 5A and B**). Moreover, ~30% of the cysts derived from Y23E-AnxA2 cells spontaneously developed into tubules In the absence of HGF.

Indeed, stimulation of three day old WT-AnxA2 cysts with HGF resulted in formation of tubules (**Fig. 5C** and **D**). Interestingly, stimulation of Y23E cells with HGF did not result in an increased formation of tubules, rather large cellular invasive complexes were formed with randomly distributed cellular protrusions; no tubules were observed at all (**Fig. 5C** and **D**). Finally, we evaluated the requirement of AnxA2 for the cyst formation and branching morphogenesis process using the pSUPER-AnxA2 cells. While control pSUPER cells formed normal cysts, AnxA2 knock down almost completely prevented cyst formation (**Fig. 5E**). Together these data indicate that while AnxA2 is essential for the organization of three dimensional cellular structures, phosphorylated AnxA2 itself can drive the branching morphogenesis process in the absence of HGF and further cooperates with HGF to induce an even more invasive branching morphogenesis phenotype.

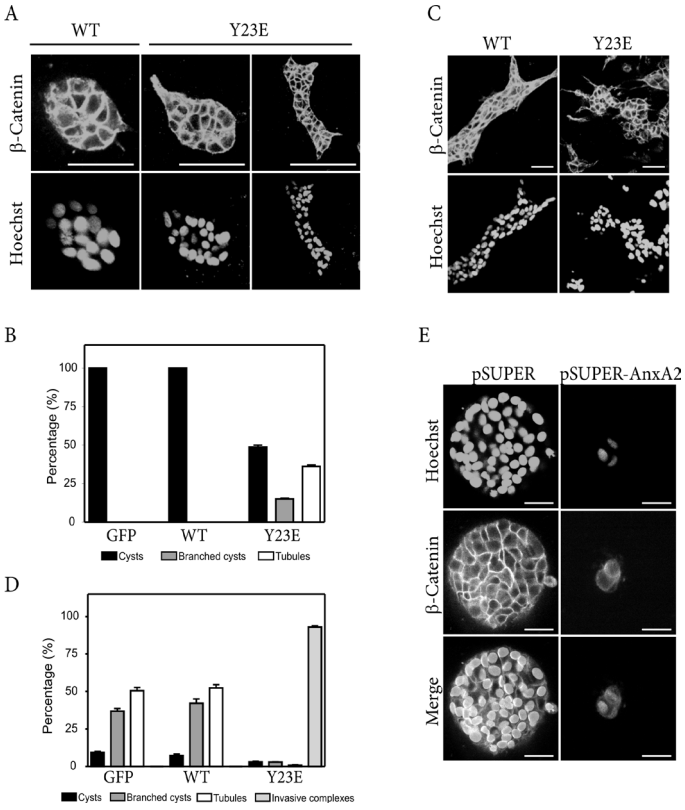

Figure 5. *Y23E-AnxA2 induces HGF-independent branching morphogenesis.* GFP, GFP-WT-AnxA2 and GFP-Y23E-AnxA2 cells were assayed for branching morphogenesis in a three-dimensional collagen type 1 gel. To determine shape of the 3D complexes, β-catenin and Hoechst staining were used. Non-stimulated cells (A) and HGF-stimulated cells (C) were analysed after 7 days of growth using confocal laser scanning microscopy. The percentages of cysts, branched complexes and tubules were calculated for non-stimulated, control cells (B) and for HGF-stimulated cells (D). pSUPER and pSUPER-shRNA-AnxA2 cells were used for a branching morphogenesis assay (E). For B and D, data represent means ± SEM of three independent experiments.

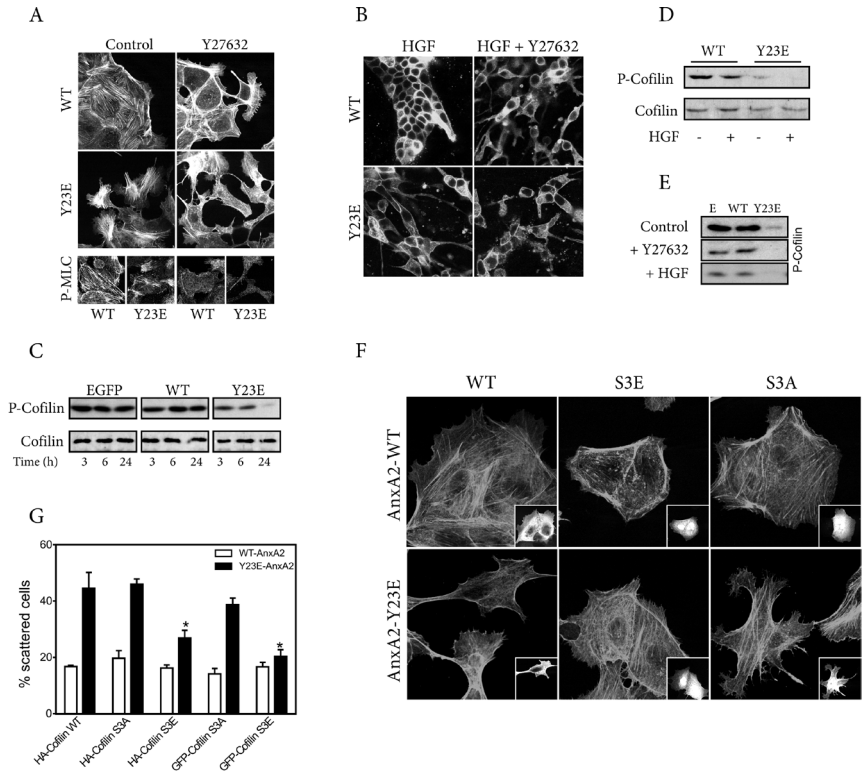

Figure 6. *Y23E-AnxA2 reorganizes the actin cytoskeleton via dephosphorylation of cofilin.* Small cell clusters were exposed to Y27632 (10 μM) to inhibit ROCK for 8 h and after fixation stained for F-actin and P-MLC (A). Cells were assayed for branching morphogenesis in a three-dimensional collagen type 1 gel as described under Materials and Methods. Cysts were exposed to HGF (50 ng/ml) in the absence or presence of Y27632 (10 μM). Multicellular structures were analysed using confocal laser scanning microscopy (B). Cells were cultured on Cn for 3, 6 or 24 h (C), in a branching morphogenesis assay (D) or treated with Y27632 or HGF for 8 h (E) and analyzed for cofilin phosphorylation using Western blotting. For (F) and (G) WT-AnxA2 and Y23E-AnxA2 cells were transiently transfected with either HA-WT-, HA-S3A or HA-S3E-cofilin, and alternatively with GFP-S3A- or GFP-S3E-cofilin. After plating on Cn overnight, cells were fixated and stained for F-actin followed by confocal laser scan microscopy imaging of the both GFP and rhodamin-phalloiding (F) and quantification of the percentage of scattered cells (G). Data are mean +/- SEM of three independent experiments.

Rho-kinase inhibition results in cell scattering and disruption of the 3D branching morphogenesis process

Rho-kinase (ROCK) is involved in the formation and contractility of stress fibers. Therefore, the absence of long and well-defined stress fibers in the Y23E-AnxA2 cells, suggests a role for phosphorylated AnxA2 in affecting the ROCK pathway. First, we determined if modulation of F-actin polymerization and contractility via ROCK inhibition could affect cell scattering. Cells were treated with Y27632, an inhibitor of Rho-kinases (ROCK)

I and II. This resulted in disruption of cell-cell interactions and an increase in cell scattering of both WT and Y23E-AnxA2 cells (**Fig. 6A**). The phosphorylation of myosin light chain (MLC), which is the main regulatory event leading to actomyosin contraction, was decreased in Y27632 treated cells (**Fig. 6A**, lower panel). P-MLC, which located along the F-actin stress fibers in WT-AnxA2 cells and was observed in F-actin clusters in Y23E-AnxA2 cells, was almost absent in Y27632 treated cells. In addition, ML-7, an MLC kinase inhibitor and blebbistatin, a myosin II ATPase inhibitor, also disrupted cell-cell junctions, further indicating that balanced cytoskeletal tension is important for the stability of AJs (data not shown).

We further evaluated how inhibition of the ROCK pathway could affect the 3D branching morphogenesis process. Y27632 together with HGF promoted formation of a completely disrupted and invasive 3D network (**Fig. 6B**) resembling that formed by Y23E-AnxA2 expression and HGF simultaneous (**Fig. 6B-D**). Although Y27632 produced very small extensions on its own, it did not cause tubule formation in the WT-AnxA2 cells by itself (data not shown), like was observed for Y23E-AnxA2 (**Fig. 6C**). These data suggest that Y23E-AnxA2 together with HGF disrupt the balance in F-actin network organization and tension which is necessary for proper branching morphogenesis.

Y23E-AnxA2-induced cell scattering is associated with dephosphorylation of cofilin and rescued by expression of a S3E cofilin mutant

Since cells treated with Y27632 share morphological changes with those induced by Y23E-AnxA2, these data suggest that Y23E-AnxA2 may affect the ROCK pathway. To further investigate the activation of the ROCK pathway, we determined the levels of cofilin phosphorylation, which is an actin-severing protein and terminal effector of the ROCK-pathway. The phosphorylation levels of cofilin were followed over time after cells were plated at low density. Phosphorylation of cofilin was lower in Y23E-AnxA2 cells compared to WT-AnxA2 cells, and almost completely absent after 24h of adhesion when Y23E-AnxA2 had obtained a scattered phenotype (**Fig. 6C**). The levels of cofilin phosphorylation in scattered Y23E-AnxA2 cells, resembled those in WT-AnxA2 cells in which scattering was induced by HGF- or the ROCK inhibitor Y27632 (**Fig. 6E**). Moreover, Y23E-AnxA2 affected the phosphorylation of cofilin in a 3D branching morphogenesis assay (**Fig. 6D**). The phosphorylation level was much lower in Y23E-AnxA2 cells compared to WT-AnxA2 cells, which further decreased in HGF treated cells.

Finally we determined the role of the cofilin phosphorylation in the Y23E-AnxA2-mediated cell scattering process. For this purpose we co-expressed either WT-cofilin, S3A-cofilin or S3E-cofilin (**Fig. 6F**). We used HA- and GFP-tagged versions of these mutants. While the S3A cofilin mutant is constitutively active and not able to be phosphorylated, the S3E cofilin mutant is constitutively inactive and mimics the phosphorylated form of cofilin. Y23E-AnxA2 cells expressing WT-cofilin obtained a scattered phenotype as untransfected cells (**Fig. 6F-G**). Also HA- as well as GFP-tagged S3A cofilin did not have an effect on the cell scattering phenotype of Y23E-AnxA2 cells. In contrast, both expression of the HA-tagged and GFP-tagged S3E-cofilin mutant inhibited efficient scat-

tering of the Y23E-AnxA2 cells which was associated with formation of cell-cell junctions (**Fig. 6F-G**). S3A-cofilin itself was not able to induce scattering in WT-AnxA2 cells. Together these observations indicate that tyrosine phosphorylation of AnxA2 on Tyr23 affects the actomyosin contractility via inhibition of the ROCK-cofilin, thus preventing substantial cofilin phosphorylation allowing a continuous dynamic actin reorganization which promotes dynamic cell protrusion formation and thus preventing efficient AJ formation.

DISCUSSION

In the present study, we have used phospho-tyrosine proteomics to identify candidate EMT modifying proteins downstream of the non-receptor tyrosine kinase Src. Tyrosine phosphorylation of the lipid-, calcium-, and actin-binding protein, annexin A2 (AnxA2) was identified as the primary phosphorylation event preceding v-Src-induced cell scattering and EMT. We assessed the biological role for AnxA2 phosphorylation on Tyr23 in the regulation of EMT-mediated processes. Our results indicate that tyrosine phosphorylation of AnxA2 1) induces F-actin reorganization and cell scattering 2) enhances cell adhesion and protrusiveness, 3) induces HGF-independent three-dimensional branching morphogenesis and 4) activates the cofilin pathway during cell scattering and branching morphogenesis. In addition, RNAi-mediated knock-down resulted in reduced cell adhesion and cell scattering, and inhibition of proper cyst formation. Together, our data suggest that tyrosine phosphorylation of AnxA2 induces reorganization of the actin stress fiber network via inhibition of the ROCK-cofilin pathway, thereby affecting cell-cell adhesion and cell scattering, which together facilitate and stimulate EMT in both two- and three dimensional cellular reorganization processes.

Our results indicate that AnxA2 phosphorylation is sufficient to induce cell scattering independently of HGF. The signalling events involved in this scattering are reminiscent of that observed for HGF and involve the activity of both PI3K and MEK [28, 26]. This suggests a close spatial and temporal relationship between AnxA2 and these signalling modalities in direct context of the actin cytoskeletal network restructuring. Indeed, AnxA2 is found at the membrane-actin cytoskeleton interface where it localizes to regions enriched in the plasma membrane lipid phosphatidylinositol-4,5-bisphosphate PtdIns(4,5)P2 [28,29] and is associated with sites of active actin remodelling, like rocketing macropinosomes [12,30], actin-rich pedestral [31] and lamellipodia [26]. Although in our hands both WT and Y23E-AnxA2 are located in lamellipodia (low density cultures) and at cell-cell junction (high density confluent monolayers), in particular the pTyr of AnxA2 affects the protein conformation, which may result in recruitment of different sets of proteins required for membrane and cytoskeletal dynamics. The architecture of the PtdIns(4,5)P2 binding site in AnxA2 is not precisely known, but depends at least in part on its unique N-terminal domain, since the C-terminal AnxA2 core domain does not efficiently compete with full-length AnxA2 for PtdIns(4,5)P2 binding [32,33]. Since Tyr 23 of AnxA2 is located within this region, phosphorylation may influence its binding to these PtdIns(4,5)P2 sites. Upon binding of AnxA2 to PtdIns(4,5)P2, clustering is observed, thereby generat-

ing spatially separated PtdIns(4,5)P2 pools [32]. Activated PI3K may subsequently convert PtdIns(4,5)P2 to PtdIns(3,4,5)P3, which is important for lamellipodia formation and actin reorganization [25]. Based on the above we propose that phosphorylated AnxA2 locally affects PtdIns (3,4,5)P3 formation, thereby driving cellular protrusiveness as observed in the Y23E-AnxA2 cells. Further research is needed to determine PtdIns (3,4,5)P3 generation and localization in Y23E-AnxA2 cells by using for example an Akt-PH-GFP sensor [34].

In addition, our data indicate a role for Tyr23 phosphorylated AnxA2 in controlling downstream Rho-kinase effectors that regulate F-actin organization and dynamics. Y23E-AnxA2 expression resulted in activation of the actin-severing protein cofilin, thereby changing actin polymerization and cytoskeletal tension and facilitating cell scattering and branching morphogenesis (**Fig. 6**). The Y23E-AnxA2-induced scattering was prevented by expression of an inactive phospho-mimicking mutant of cofilin (**Fig. 6E-F**), suggesting a critical role for cofilin in AnxA2-dependent cell scattering. The maintenance of a balanced cytoskeletal tension is important for formation of tissue [35] and branching morphogenesis [36]. We reason that Y23E-AnxA2-induced cofilin dephosphorylation resulted in branching morphogenesis in the absence of HGF, while a further decrease in cytoskeletal tension by the addition of HGF results in a disturbance of proper branching. Moreover, actin polymerization is important for the recruitment and maintenance of AJ proteins at cell-cell contacts [33,37]. Genetic elimination of actin-binding proteins or overexpression of mutant junctional proteins lacking actin-binding sites impairs the formation of epithelial AJs [37,38]. Thus, tension generated by the actin cytoskeleton is essential for correct AJ assembly, suggesting that the inhibition of cell-cell junction formation in Y23E-AnxA2 cells is due to the disturbance in cytoskeletal tension. Together our data support the idea that tensional homeostasis via balanced F-actin polymerization/depolymerisation processes is important for proper AJ assembly and branching morphogenesis processes [26].

How might Y23E-AnxA2 affect the cofilin pathway? Actin depolymerizing components, including proteins of the cofilin/ADF family, disassemble F-actin from the rear of the actin network to recycle actin monomers to the leading edge for further rounds of polymerization. Cofilin is unable to bind actin in its phosphorylated form and dephosphorylation of Ser3 reactivates the actin-depolymerization activity of cofilin [32,38]. Hayes *et. al.* showed that AnxA2 can bind and sequester G-actin, as has been reported for cofilin, thereby regulating actin filament turnover, most likely through monomer sequestration and barbed-end capping activities [38,39]. However, AnxA2 has the extra ability to bind to the plasma-membrane, and might therefore be capable of delivering monomers directly to the cell cortex, where they are required for rapid polymerization.

Here we studied in detail the cell biological role of AnxA2 phosphorylation. Our proteomics data indicate that the actin binding proteins AnxA1 and A2, are among the first proteins phosphorylated in relation to Src kinase activation (**Fig. 1C** and data not shown). AnxA1 is directly phosphorylated by the epidermal growth factor (EGF) receptor, whereas AnxA2 is phosphorylated by Src kinase [10]. While in this study we demon-

strate a role of AnxA2 phosphorylation in the control of cofilin coordinated reorganization of the actin cytoskeletal network prior to the EMT, the combined phosphorylation of AnxA1 and AnxA2 may well be required in growth factor stimulated cell scattering and/or three dimensional reorganization of cellular structures.

Together our data show that phosphorylation of AnxA2 plays an important role in the regulation of F-actin cytoskeletal dynamics, via activation of the cofilin pathway, thereby facilitating EMT-related processes in both 2D- and 3D-culture models. Since the activation of cofilin is linked to invasion and metastasis of tumors [36] and AnxA2 expression is elevated in a subset of mesenchymal breast tumor cells (de Graauw *et. al.*, Cleton and van de Water, unpublished observations), phosphorylation of AnxA2 play a role in tumor metastasis formation.

ACKNOWLEDGEMENTS

We thank Dr. V. Gerke and U. Rescher for the AnxA2 constructs and antibodies, Flip Deen for the Sypro ruby staining solution, Danny Burg for help with the siRNA constructs and Erik Danen and other members of the division of Toxicology of the LACDR for valuable discussion and critically reading the manuscript. This work was supported by grants from the Netherlands Organization for Scientific Research (grants 902-21-229 and 911-02-022). BvdW was supported by a fellowship of the Royal Netherlands Academy for Arts and Sciences.

REFERENCE LIST

1. Thiery, J. P. Epithelial-mesenchymal transitions in tumour progression. Nat.Rev.Cancer, 2: 442-454, 2002.

2. Zeisberg, M. and Kalluri, R. The role of epithelial-to-mesenchymal transition in renal fibrosis. J.Mol.Med., 82 : 175-181, 2004.

3. O'Brien, L. E., Zegers, M. M., and Mostov, K. E. Opinion: Building epithelial architecture: insights from three-dimensional culture models. Nat.Rev.Mol.Cell Biol., 3: 531-537, 2002.

4. Rahimi, N., Hung, W., Tremblay, E., Saulnier, R., and Elliott, B. c-Src kinase activity is required for hepatocyte growth factor-induced motility and anchorage-independent growth of mammary carcinoma cells. J.Biol.Chem., 273: 33714-33721, 1998.

5. Behrens, J., Vakaet, L., Friis, R., Winterhager, E., Van Roy, F., Mareel, M. M., and Birchmeier, W. Loss of epithelial differentiation and gain of invasiveness correlates with tyrosine phosphorylation of the E-cadherin/beta-catenin complex in cells transformed with a temperature-sensitive v-SRC gene. J.Cell Biol., 120: 757-766, 1993.

6. Heiska, L. and Carpen, O. Src phosphorylates ezrin at tyrosine 477 and induces a phospho-specific association between ezrin and a kelch-repeat protein family member. J.Biol.Chem., 280: 10244-10252, 2005.

7. Sefton, B. M., Hunter, T., Ball, E. H., and Singer, S. J. Vinculin: a cytoskeletal target of the transforming protein of Rous sarcoma virus. Cell, 24: 165-174, 1981.

8. Gerke, V., Creutz, C. E., and Moss, S. E. Annexins: linking Ca2+ signalling to membrane dynamics. Nat.Rev.Mol.Cell Biol., 6: 449-461, 2005.

9. Gould, K. L., Woodgett, J. R., Isacke, C. M., and Hunter, T. The protein-tyrosine kinase substrate p36 is also a substrate for protein kinase C in vitro and in vivo. Mol.Cell Biol., 6: 2738-2744, 1986.

10. Radke, K. and Martin, G. S. Transformation by Rous sarcoma virus: effects of src gene expression on the synthesis and phosphorylation of cellular polypeptides. Proc.Natl.Acad.Sci. U.S.A, 76: 5212-5216, 1979.

11. Knop, M., Aareskjold, E., Bode, G., and Gerke, V. Rab3D and annexin A2 play a role in regulated secretion of vWF, but not tPA, from endothelial cells. EMBO J., 23: 2982-2992, 2004.

12. Hayes, M. J., Shao, D., Bailly, M., and Moss, S. E. Regulation of actin dynamics by annexin 2. EMBO J., 25: 1816-1826, 2006.

13. Mayran, N., Parton, R. G., and Gruenberg, J. Annexin II regulates multivesicular endosome biogenesis in the degradation pathway of animal cells. EMBO J., 22: 3242-3253, 2003.

14. Yamada, A., Irie, K., Hirota, T., Ooshio, T., Fukuhara, A., and Takai, Y. Involvement of the annexin II-S100A10 complex in the formation of E-cadherin-based adherens junctions in Madin-Darby canine kidney cells. J.Biol.Chem., 280: 6016-6027, 2005.

15. Zobiack, N., Rescher, U., Ludwig, C., Zeuschner, D., and Gerke, V. The annexin 2/S100A10 complex controls the distribution of transferrin receptor-containing recycling endosomes. Mol. Biol.Cell, 14: 4896-4908, 2003.

16. Shadle, P. J., Gerke, V., and Weber, K. Three Ca2+-binding proteins from porcine liver and intestine differ immunologically and physicochemically and are distinct in Ca2+ affinities. J.Biol.Chem., 260: 16354-16360, 1985.

17. Alvarez-Martinez, M. T., Mani, J. C., Porte, F., Faivre-Sarrailh, C., Liautard, J. P., and Sri, W. J. Characterization of the interaction between annexin I and profilin. Eur.J.Biochem., 238: 777-784, 1996.

18. Filipenko, N. R. and Waisman, D. M. The C terminus of annexin II mediates binding to F-actin. J.Biol.Chem., 276: 5310-5315, 2001.

19. Thiel, C., Osborn, M., and Gerke, V. The tight association of the tyrosine kinase substrate annexin II with the submembranous cytoskeleton depends on intact p11- and Ca(2+)-binding sites. J.Cell Sci., 103: 733-742, 1992.

20. Hubaishy, I., Jones, P. G., Bjorge, J., Bellagamba, C., Fitzpatrick, S., Fujita, D. J., and Waisman, D. M. Modulation of annexin II tetramer by tyrosine phosphorylation. Biochemistry, 34: 14527-14534, 1995.

21. de Graauw, M., Tijdens, I., Cramer, R., Corless, S., Timms, J. F., and van de Water, B. Heat shock protein 27 is the major differentially phosphorylated protein involved in renal epithelial cellular stress response and controls focal adhesion organization and apoptosis. J.Biol. Chem., %19;280: 29885-29898, 2005.

22. Giaever, I. and Keese, C. R. A morphological biosensor for mammalian cells. Nature, 366: 591-592, 1993.

23. Glenney, J. Two related but distinct forms of the Mr 36,000 tyrosine kinase substrate (calpactin) that interact with phospholipid and actin in a Ca2+-dependent manner. Proc.Natl. Acad.Sci.U.S.A, 83: 4258-4262, 1986.

24. Khwaja, A., Lehmann, K., Marte, B. M., and Downward, J. Phosphoinositide 3-kinase induces scattering and tubulogenesis in epithelial cells through a novel pathway. J.Biol.Chem., 273: 18793-18801, 1998.

25. Oikawa, T., Yamaguchi, H., Itoh, T., Kato, M., Ijuin, T., Yamazaki, D., Suetsugu, S., and Takenawa, T. PtdIns(3,4,5)P3 binding is necessary for WAVE2-induced formation of lamellipodia. Nat.Cell Biol., 6: 420-426, 2004.

26. Royal, I. and Park, M. Hepatocyte growth factor-induced scatter of Madin-Darby canine kidney cells requires phosphatidylinositol 3-kinase. J.Biol.Chem., 270: 27780-27787, 1995.

27. Rosario, M. and Birchmeier, W. How to make tubes: signalling by the Met receptor tyrosine kinase. Trends Cell Biol., 13: 328-335, 2003.

28. Hayes, M. J., Merrifield, C. J., Shao, D., Ayala-Sanmartin, J., Schorey, C. D., Levine, T. P., Proust, J., Curran, J., Bailly, M., and Moss, S. E. Annexin 2 binding to phosphatidylinositol 4,5-bisphosphate on endocytic vesicles is regulated by the stress response pathway. J.Biol.Chem., 279: 14157-14164, 2004.

29. Rescher, U., Ruhe, D., Ludwig, C., Zobiack, N., and Gerke, V. Annexin 2 is a phosphatidylinositol (4,5)-bisphosphate binding protein recruited to actin assembly sites at cellular membranes. J.Cell Sci., 117: 3473-3480, 2004.

30. Merrifield, C. J., Rescher, U., Almers, W., Proust, J., Gerke, V., Sechi, A. S., and Moss, S. E. Annexin 2 has an essential role in actin-based macropinocytic rocketing. Curr.Biol., 11: 1136-1141, 2001.

31. Zobiack, N., Rescher, U., Laarmann, S., Michgehl, S., Schmidt, M. A., and Gerke, V. Cell-surface attachment of pedestal-forming enteropathogenic E. coli induces a clustering of raft components and a recruitment of annexin 2. J.Cell Sci., 115: 91-98, 2002.

32. Gokhale, N. A., Abraham, A., Digman, M. A., Gratton, E., and Cho, W. Phosphoinositide specificity of and mechanism of lipid domain

formation by annexin A2-p11 heterotetramer. J.Biol.Chem., 280: 42831-42840, 2005.

33. Miyake, Y., Inoue, N., Nishimura, K., Kinoshita, N., Hosoya, H., and Yonemura, S. Actomyosin tension is required for correct recruitment of adherens junction components and zonula occludens formation. Exp.Cell Res., 312: 1637-1650, 2006.

34. Menager, C., Arimura, N., Fukata, Y., and Kaibuchi, K. PIP3 is involved in neuronal polarization and axon formation. J.Neurochem., 89: 109-118, 2004.

35. Moore, K. A., Polte, T., Huang, S., Shi, B., Alsberg, E., Sunday, M. E., and Ingber, D. E. Control of basement membrane remodeling and epithelial branching morphogenesis in embryonic lung by Rho and cytoskeletal tension. Dev.Dyn., 232: 268-281, 2005.

36. Yu, W., O'Brien, L. E., Wang, F., Bourne, H., Mostov, K. E., and Zegers, M. M. Hepatocyte growth factor switches orientation of polarity and mode of movement during morphogenesis of multicellular epithelial structures. Mol.Biol. Cell, 14: 748-763, 2003.

37. Vasioukhin, V. and Fuchs, E. Actin dynamics and cell-cell adhesion in epithelia. Curr. Opin.Cell Biol., 13: 76-84, 2001.

38. Bershadsky, A. Magic touch: how does cell-cell adhesion trigger actin assembly? Trends Cell Biol., 14: 589-593, 2004.

39. Wozniak, M. A. and Keely, P. J. Use of three-dimensional collagen gels to study mechanotransduction in T47D breast epithelial cells. Biol.Proced.Online., 7: 144-161, 2005.